Comparison of Seismic Responses of Geosynthetically Reinforced Walls with Tire-Derived Aggregates and Granular Backfills

Ming Xiao, M.ASCE[1]; Jan Bowen[2]; Mathew Graham[3]; and Jesus Larralde, M.ASCE[4]

Abstract: This paper reports the seismic responses of geosynthetically reinforced walls with two types of backfills using shake table tests. The backfills are tire-derived aggregates (TDA) and poorly graded sand, respectively. Mechanically stabilized earth (MSE) walls with reinforced TDA backfill have not been fully tested under seismic conditions. In this study, two geosynthetically reinforced walls are tested on a one-dimensional shake table. A section of reduced-scale MSE wall (1.6 m high, 1.5 m deep, and 1.5 m long) is built in a box that is anchored on a shake table that can generate earthquake excitations obtained from actual field recordings. Layers of geogrid are used as reinforcement. The geosynthetic reinforcement is based on static external and internal stability design. In each test, the segmental MSE wall is instrumented with accelerometers, linear variable differential transformers, linear potentiometers, and dynamic soil stress gauges to record the accelerations, wall vertical deformations, horizontal deflections of the wall face, and transient effective stresses during the shaking, respectively. The experimental study reveals the advantageous seismic performances of a geosynthetically reforced wall with TDA backfill over an MSE wall using traditional granular backfill. **DOI: 10.1061/(ASCE)MT.1943-5533.0000514.**

CE Database subject headings: Tires; Aggregates; Seismic effects; Shake table tests; Backfills; Geosynthetics.

Author keywords: Tirederived aggregates; Mechanically stabilized earth walls; Seismic responses; Shake table tests.

Introduction

As the nation's highway and bridge infrastructure age, the necessity of repairing and replacing them often means more traffic congestion. According to the Federal Highway Administration (FHWA 2006), vehicle miles of travel increased by 80% and licensed drivers increased by 31% from 1980 to 2000. Meanwhile, lane miles increased only by 3.8%, and over 40% of all bridges are more than 40 years old, with a design life of 50 years when they were built. Although highway construction is unavoidable, excessive construction time must be minimized because it is costly, exposes highway workers to traffic, and burdens motorists to prolonged substandard conditions. To prevent this gridlock and to preserve and maintain the highway system with the least impact on the motoring public, accelerated construction techniques are gaining popularity across the country. The FHWA has been actively promoting the advantages of accelerated bridge construction (ABC). The annual reports of the Accelerated Construction Technology Transfer of the FHWA (ACTT 2005, 2006, 2007) recommended a variety of accelerated construction techniques, such as using mechanically stabilized earth (MSE) walls and utilizing alternative accelerated backfills, such as recycled materials or flowable backfills. These backfills usually do not need moistening or compaction, and thus shorten the construction time.

Over the past decade, the MSE technology has been applied to bridge-supporting structures. They are similar in principle to MSE retaining walls, except that MSE abutments are typically subjected to much higher loads, and these loads are close to the wall face. The MSE abutments are easier to construct, more economical than their conventional counterparts—reinforced concrete abutments—and can eliminate the use of piles over weak foundations. This technique will not only reduce costs, but can also lessen the differential settlements of the bridge approach often experienced at the ends of the bridge resting on a pile-supported foundation (Helwany et al. 2007). Coupled with accelerated backfill technology, the MSE abutment construction may gain wide popularity in the sustainable infrastructure, especially in relation to accelerated bridge construction.

One type of recycled material that has gained attention in the past two decades is waste tire. The FHWA (1997) estimated that approximately 280 million tires are discarded each year by American motorists, 40% of which are disposed in landfills, stockpiles, or illegal dumps. In California, approximately 44.8 million reusable and waste tires are generated annually, with a fewer than 250,000 waste tires remaining in stockpiles throughout California (CalRecycle 2010). These stockpiles pose a potential threat to public health, safety, and the environment. Tire shreds, also known as tire-derived aggregates (TDA), are pieces of processed and shredded waste tires that can be used as lightweight and quick fills for embankments, subgrades, bridge abutments, and retaining wall backfills. Constructed on weak and compressible foundation soils, bridge abutments using tire shreds that are reinforced with geosynthetics result in less overburden pressure, efficient drainage, and more economical costs.

[1]Associate Professor, Dept. of Civil and Geomatics Engineering, M/S EE94, California State Univ., Fresno, CA 93740 (corresponding author). E-mail: mxiao@csufresno.edu

[2]Graduate student, Dept. of Civil and Geomatics Engineering, M/S EE94, California State Univ., Fresno, CA 93740.

[3]Graduate student, Dept. of Civil and Geomatics Engineering, M/S EE94, California State Univ., Fresno, CA 93740.

[4]Professor, Dept. of Civil and Geomatics Engineering, M/S EE94, California State Univ., Fresno, CA 93740.

Note. This manuscript was submitted on August 6, 2011; approved on March 7, 2012; published online on March 10, 2012. Discussion period open until April 1, 2013; separate discussions must be submitted for individual papers. This paper is part of the ***Journal of Materials in Civil Engineering***, Vol. 24, No. 11, November 1, 2012. © ASCE, ISSN 0899-1561/2012/11-1368-1377/$25.00.

J. Mater. Civ. Eng. 2012.24:1368-1377.

TDAs of different sizes have been widely studied as alternative backfills for the past twenty years and vast literature references are available (Humphrey and Manion 1992; Humphrey 1998; Bosscher et al. 1992; Tweedie et al. 1998; Strenk et al. 2007; Tandon et al. 2007). These studies offer expanded knowledge on the mechanical characteristics and in situ performance of embankments or retaining walls using tire shreds or chips. In a recent study, Pando and Garcia (2011) summarized the shear strengths of TDA of various sizes (2 to 13 mm) under various confining pressures obtained by previous researchers; moreover, based on their study, they reported the ranges of effective cohesion (0–14 kPa) and effective friction angle (14.9–9.2°) of TDA of maximum size of 4.5 mm when the TDA is subjected to confining pressures ranging from 25 to 100 kPa at 20% strain. A mixture of shredded tires and sand is another popular backfill alternative and its static responses (stress, deformation, and strength) have also been investigated (Foose et al. 1996; Bosscher et al. 1997; Lee et al. 1999; Wartman et al. 2007). The static performances of conventional cantilever retaining walls using TDA and sand as backfills were also studied. Pando and Garcia (2011), based on their model tests and centrifuge experiments, concluded that (1) lateral pressures induced by TDA backfills tend to be smaller than predicted using the conventional earth pressure theories in active and at-rest conditions; (2) levels of wall movement required to reach active and passive conditions are different from the typical values observed using conventional mineral soil backfills; and (3) active Rankine earth pressure coefficient for TDA is approximately 29% lower than using conventional silica sand backfill. Their study revealed the advantageous performances of TDA walls over the retaining walls using sand backfill at static conditions; meanwhile, it shows that the traditional retaining wall design methodologies may not adequately reflect the performances of TDA walls and abutments in the field.

In contrast to the relatively rich literature on the static behaviors of tire shreds, scarce experimental data are available on the seismic performances of mechanically stabilized walls and bridge abutments with tire shreds/chips as backfills. Tsang (2008) is one of few researchers who studied a rubber-soil mixture backfill under seismic conditions. In shake table tests, it was found that site response of the backfill was nonlinear and helped absorb incident seismic waves. Furthermore, Tsang (2008) raised the concern for the resonance effects of the new backfill, which should be experimentally tested. The recent shake table tests on gravity type model caisson protected by a cushioning tire chips found that the tire chips substantially reduced the seismic load against the caisson wall (Hazarika et al. 2008).

Reinforced segmental retaining walls have shown advantages of safety, environmental friendliness, and savings in labor costs, equipment, and time. They generally performed well (no evidence of visual damage or with only minor damage) during the past major earthquakes, such as the 1994 Northridge earthquake ($M = 6.7$) (Sandri 1994), the 1989 Loma Prieta earthquake ($M = 7.1$) (Eliahu and Watt 1991; Collin et al. 1992), and the 1995 Kobe earthquake ($M = 6.9$) (Tatsuoka et al. 1996). However, major repairs or complete collapses were also reported for some MSE walls in the 1999 Chi-Chi earthquake ($M = 7.6$) (Huang and Tatsuoka 2001; Ling et al. 2001) and in the 1995 Kobe earthquake (Tatsuoka et al. 1997). With the innovative backfill alternatives for accelerated bridge construction, the mechanically stabilized walls or bridge abutments have yet to be fully tested and understood under seismic conditions. The transient seismic pressure of the new fill materials on the modular facing, the dynamic settlement, the horizontal deflection of wall face, and the time response of horizontal accelerations during earthquakes are unknown, and therefore are the focuses in this research.

The objectives of this research project are to compare the seismic behaviors of mechanically stabilized walls using TDA and sand backfills and to investigate the feasibility of using TDA as a quick backfill alternative in MSE wall construction.

Materials, Experimental Setup, and Instrumentation

The MSE walls are constructed and tested on a shake table, which is housed in the Structural Laboratory in the Lyles College of Engineering at Fresno State. The table replicates ground motions that may be observed in actual earthquakes. The dimensions of the shaking table are 2.44×2.13 m (8×7 ft), and the load capacity is 177.9 kN (20.0 tons). The table is driven in one dimension by a 100 gallons-per-minute (gpm) pump and an actuator that provides a 245-kN (55 kips) hydraulic fluid driving force through a 25.4-cm (10 in.) displacement stroke. A steel-reinforced box, as shown in Fig. 1, is built and anchored on the shake table. The frame of the box is designed and built to be rigid, so that it moves with the same displacement and accelerations of the shake table. The box has inside dimensions of 186 cm (73.5 in.) length in the shaking direction, 168 cm (66 in.) width, and 183 cm (72 in.) height. Three walls of the box are made of 2.54-cm (1.0 in.) thick plywood and the fourth wall is made of 1.27 cm (0.5 in.) thick transparent polycarbonate sheet, so that the MSE wall's responses during a seismic shaking can be visually recorded.

Two backfill materials are used. One is TDA that are manufactured by West Coast Rubber Recycling (Gilroy, CA); the nominal size is 15.2 cm (6 in.). The TDA has exposed steel beltings. The other is a poorly graded sand with no clay. Fig. 2 shows the size distributions of both materials. To obtain the size distribution of the TDA, five gallons (or 18, 927 cm^3) of the TDA are randomly picked from the batch. Each TDA piece has the length (longest), width (intermediate), and thickness (smallest) dimensions. In this research, the longest length of each TDA piece is measured and taken as its size; then, its mass is measured. If using sieve analysis, the TDA pieces can lay flat or vertical. If flat, the length is the measured dimension; if vertical, the width is the measured dimension. Therefore, the measured size distribution using sieve analysis could shift to the right of the TDA size distribution in Fig. 2. The bulk density of the TDA is 529 kg/m^3 (33 lb/ft^3). For the sand backfill, the poorly graded sand is initially moistened at 4% and compacted

Fig. 1. Shake table test of seismic responses of MSE walls

J. Mater. Civ. Eng. 2012.24:1368-1377.

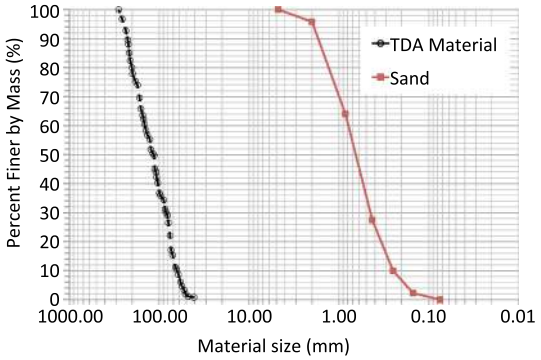

Fig. 2. Size distributions of TDA and sand

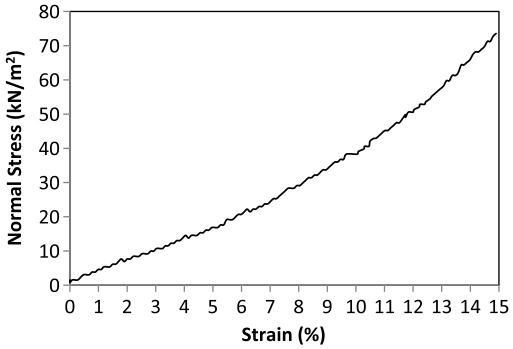

Fig. 4. Static stress-strain curve of the TDA

to 90% of the maximum dry density, 1,630 kg/m^3 or 102 lb/ft^3, based on the Modified Proctor Test.

To understand the mechanical properties of the TDA material, a compression test is conducted, as shown in Fig. 3. The TDA is contained in a wooden box of 112 cm length, 71 cm width, and 88 cm height. The thickness of the TDA in the box is 50 cm. Two loading plates are positioned on the TDA surface to simulate a surcharge of 3.19 kN/m^2. This surcharge is similar to that (3.38 kN/m^2) applied on the model MSE walls in this research. The stress-strain curve of the TDA is shown in Fig. 4. An apparent upswing of the strain-stress curve is observed, indicating a stiffer behavior of the TDA material. The tested TDA material has an initial bulk density of 529 kg/m^3 (33 lb/ft^3). As the TDA material becomes condensed during the compression in the confined box, increased density of the TDA may cause the stiffening trend of the material.

Fig. 5 shows the details of the MSE wall configuration and instrumentation. Both backfills have the same test configuration. The wall is 1.60 m tall (63 in.), 1.68 m (66 in.) wide, and the horizontal depth (in the shaking direction) is 1.50 m (59 in.). A 10-cm (3.9 in.) sand layer is compacted beneath the wall to simulate the base soil. The wall is made of four layers and geogrid is used as the reinforcement [Fig. 6(a)]. Two types of geogrid are used together: uniaxial and biaxial. The geogrid installation follows the field practice recommended by Tensar Inc. The biaxial geogrid wraps around each layer and provides the tensile strength and internal stability; the uniaxial geogrid is laid only at the bottom of each backfill layer, but above the biaxial geogrid. The formwork and the geogrid are first installed before the compaction, as shown in Fig. 6(a). It is observed that TDA is not compactable; compaction forces only temporarily compress the TDA, which rebounds after the compression force is removed. Therefore, the TDA is dumped into the box using a crane and leveled using shovels, then two people simply step evenly on the TDA. For sand backfill, a 15-kg hand hammer with a long handle and 30 × 30 cm steel base is used to compact the pre-moistened sand. Figure 6(b) shows the finished MSE wall with TDA as backfill. To simulate the surcharge on the MSE wall, a concrete slab of 15 cm in thickness is anchored on top of the backfill, providing a uniform pressure of 3.38 kN/m^2 (70.6 lb/ft^2) [Fig. 6(c)].

Fig. 3. Experimental setup of TDA compression test

As shown in Figs. 1 and 5, four linear potentiometers are used to measure the horizontal deflections of the wall face at different elevations. The potentiometers are fixed on an inertial frame outside of the shake table, and an inelastic wire connects to each potentiometer and to the geogrid of each layer. The potentiometers are spring loaded, but the spring force is significantly smaller than the seismic force, therefore, the spring stiffness does not affect the responses of the walls. The vertical deformation of the MSE wall during the shaking is measured using LVDT transducers that are anchored on the shake table above the concrete slab [Fig. 6(c)]. The transient effective stresses in the backfill are measured by Geokon's dynamic soil pressure cells, which are laid flat at the bottom of each layer [Fig. 6(a)]. The accelerations during the shaking are measured by wire-free accelerometers, with two per layer: one close to the wall face (referred to as front backfill), and one away from the wall surface (referred to as back backfill). The top layer only has one accelerometer in the front backfill. The accelerometers are not wired to avoid the interferences that might be caused by a wire during the shaking. A timer is set in each accelerometer and the data recording (100 data per second) starts at a predetermined time when the shake table test is run. The instrumentations are connected to the National Instrument data acquisition system that is located outside of the shake table. Two high-definition camcorders are used to visually record the seismic behaviors: one is positioned above the MSE wall and the other faces the transparent polycarbonate sidewall.

Test Program

The shake table uses the combined earthquake excitations of the 1940 El Centro earthquake and the 1994 Northridge earthquake.

J. Mater. Civ. Eng. 2012.24:1368-1377.

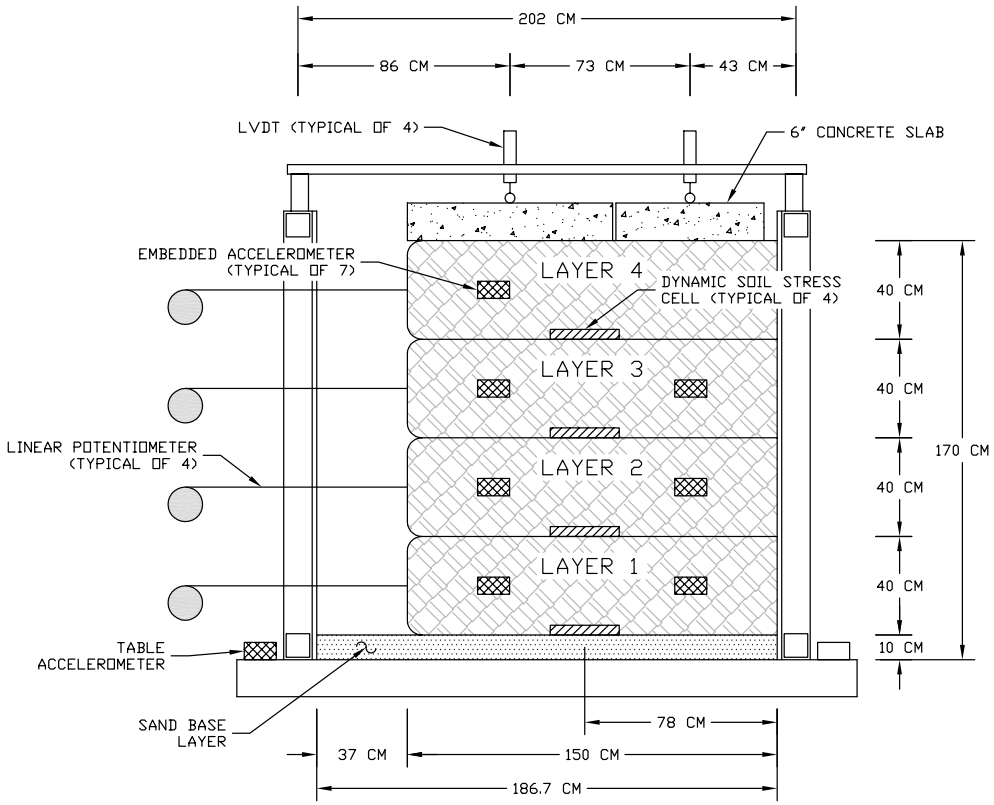

Fig. 5. Test configurations

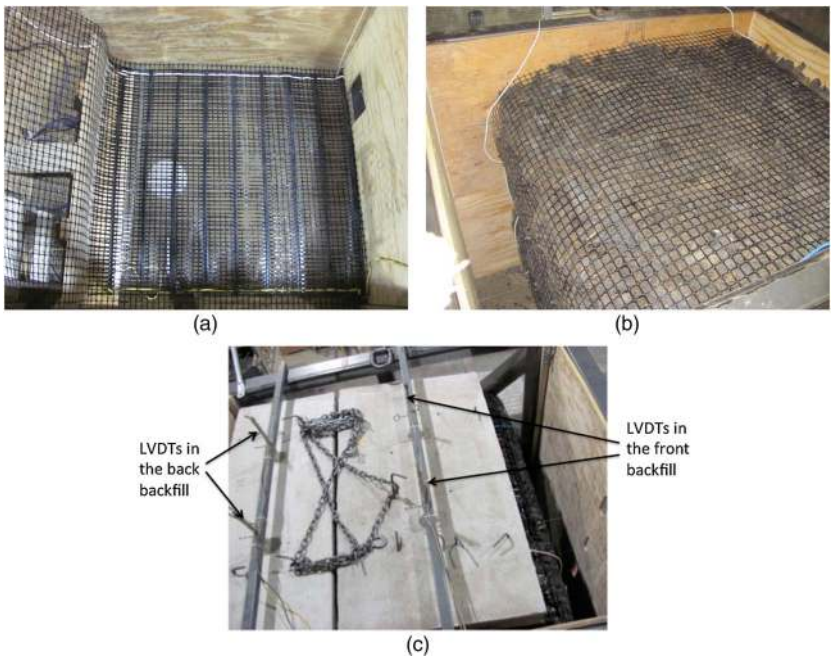

Fig. 6. Geogrid reinforced wall construction: (a) construction of MSE wall (backfill is sand); (b) before the placement of concrete slab (backfill is TDA); (c) after the placement of concrete slab, which simulates the surcharge on the MSE wall

The input file to the MTS® control system of the shake table is in terms of displacement versus time. The two earthquake excitations are sequentially combined into one input file, which controls the actuator that pushes or pulls the shake table using the specified displacement time history. Fig. 7 shows response spectra of the input motion, which is the displacement versus time relationship of the shake table. The modified one-dimensional intense shaking is 17 s long. Two tests are conducted using the TDA and sand as

J. Mater. Civ. Eng. 2012.24:1368-1377.

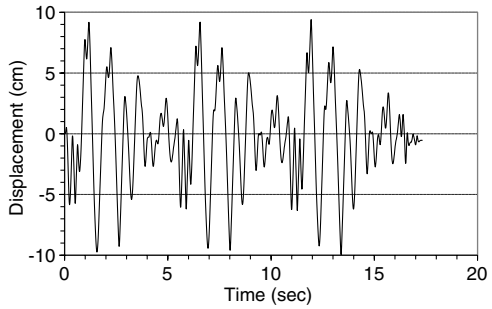

Fig. 7. Shake table displacement versus time history

backfills, respectively. Except for the backfills, the test configuration, instrumentation, and shaking are identical for both tests. The measured acceleration response time histories of the box during the two shake table tests are graphed in Figs. 8(a and b). The accelerometer in each test is mounted on the box, not on the shake table, and Fig. 8 shows that the two boxes' acceleration response spectra are different. Although the shake table provides the same excitation, the rigid box on the table responds differently, which is attributable to the weight difference of the sand and TDA backfills in the box. The Northridge earthquake ground acceleration was one of the highest ever instrumentally recorded in an urban area in the North America, measuring 1.7 g. The accelerations produced by the shake table are high, as shown in the figures. A few outliers of the acceleration data are outside of the range of ±2 g; they are likely caused by the forceful cycling movement of the actuator, and are not believed to represent the realistic ground motions. This research focuses on the comparison of the two MSE walls' seismic responses under the same shaking. Therefore, the limitation of the unrealistic shake table excitations is ignored.

Results and Discussion

Lateral displacements of the wall face, vertical settlement of the MSE wall surface, accelerations of the four layers within the MSE wall, and dynamic vertical stresses of the four layers within the MSE wall are presented in this section.

Fig. 9 shows the lateral displacements of the four layers of the TDA wall face, relative to the shake table movement, i.e., the absolute movements of the four layers recorded by the linear potentiometers minus the absolute movements of the shake table at the same time stamps. The graph shows the expected increasing trend of lateral displacement toward the top of the wall, with the highest displacement close to 30 cm (11.8 in.), indicating a rotational failure of the wall. To understand the relative displacement of each layer with respect to the underlying layer of the mechanically stabilized TDA wall, the absolute displacements of each layer minus the absolute displacement of its immediately underlying layer are graphed in Fig. 10. This information can be used to evaluate the damage that can be caused to the MSE wall facing by the relative lateral displacements. The most prominent relative displacement is from the bottom layer against the shake table, which simulates the ground movement. The second largest lateral displacement is from the top layer. The middle layers (layers 2 and 3) have the least displacement. Table 1 lists the maximum lateral displacements of the four layers of the MSE walls with TDA and sand backfills, respectively. Figs. 11 and 12 show the lateral displacement data of the mechanically stabilized sand wall in the same formats with the

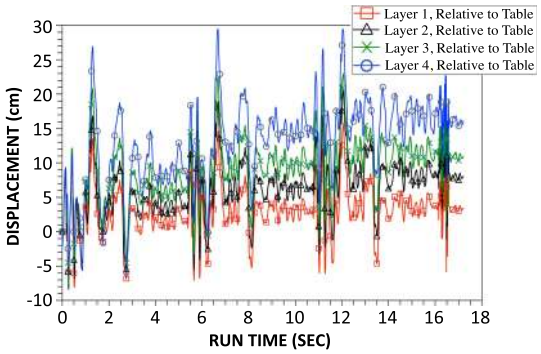

Fig. 9. Lateral displacements of TDA wall face, relative to table movement (layer 1 is the bottom layer; layer 4 is the top layer)

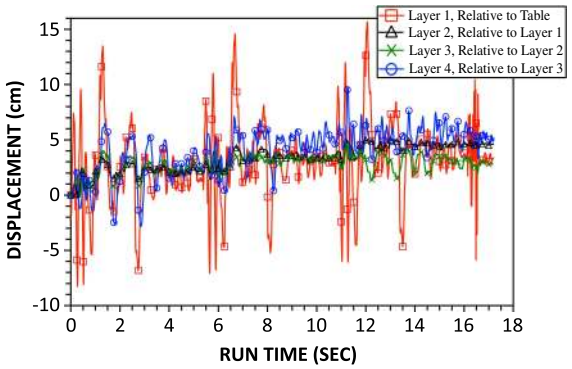

Fig. 10. Lateral displacements of TDA wall face, relative to underlying layer (layer 1 is the bottom layer; layer 4 is the top layer)

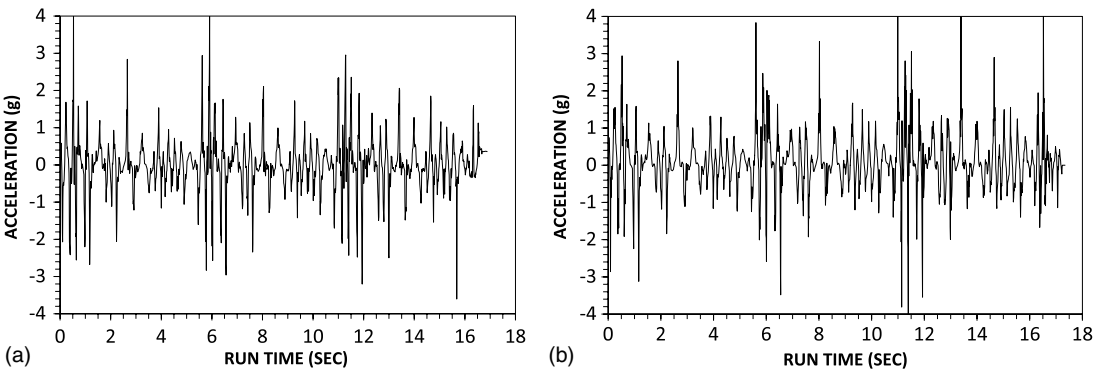

Fig. 8. Accelerations versus time history of the box: (a) TDA as backfill; (b) sand as backfill

J. Mater. Civ. Eng. 2012.24:1368-1377.

Table 1. Maximum Lateral Displacements of the MSE walls with TDA and Sand Backfills

Locations of displacements	TDA backfill, relative to table movement	Sand backfill, relative to table movement	TDA backfill, relative to underlying layer	Sand backfill, relative to underlying layer
Layer 4 (top)	29.5 (11.6)	41.5 (16.3)	9.7 (3.8)	12.5 (4.9)
Layer 3	23.0 (9.1)	34.6 (13.6)	5.0 (2.0)	8.0 (3.1)
Layer 2	20.6 (8.1)	34.6 (13.6)	5.0 (2.0)	9.0 (3.5)
Layer 1 (bottom)	15.7 (6.2)	25.2 (9.9)	15.7 (6.2)	25.2 (9.9)

Note: The values are presented in both cm and in., with the English units in parentheses.

same trends. The maximum displacement relative to the shake table is from the top layer (layer 4), which is 41% more than the TDA wall. The relative displacements with respect to the underlying layer in the MSE sand wall are also larger than the TDA wall, with the largest relative lateral displacement at 60% more than the TDA wall.

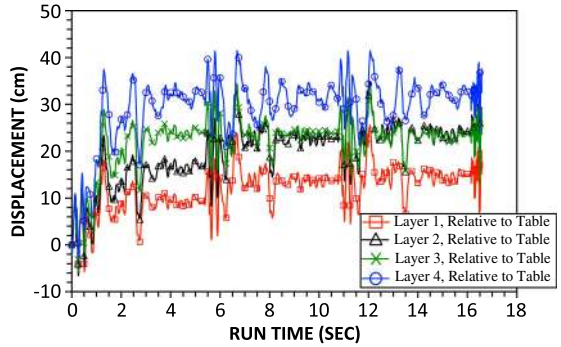

Fig. 11. Lateral displacements of sand wall face, relative to table movement

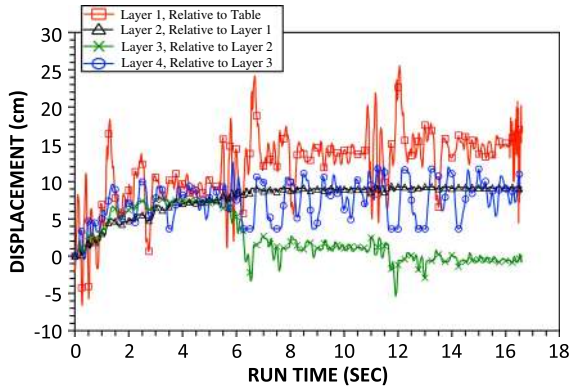

Fig. 12. Lateral displacements of sand wall face, relative to underlying layer

Fig. 13 shows the vertical settlements of the two geosynthetically reinforced walls during the 17 s of shaking, and the settlements are recorded by the LVDT transducers. Fig. 6(c) shows that there are two LVDTs on the front and back backfills, respectively, for duplication purpose. Fig. 13 only shows the readings of one LVDT for each back and front backfill. The inner LVDT rod is 13 cm (5.1 in.) long; if the settlement is more than 13 cm, the rod drops out of the LVDT tube and no reading can be recorded, as is the case in the back backfill of the TDA wall and for both back and front backfills of the sand MSE wall. The graphs clearly show much larger and faster dynamic settlements of the sand retaining wall than the TDA retaining wall. Fig. 13(a) shows that the settlement of the TDA wall closer to the simulated bridge deck has less than 6 cm (2.4 in.) settlement during the entire extensive shaking, much less than the sand MSE wall. In the sand MSE wall, the LVDT rods fall out of the LVDT tubes, indicating that the vertical settlements are larger than 13 cm. Therefore, the dynamic settlement of the sand wall is over 100% more than that of the TDA wall. Another observation is the upward heaving of the TDA backfill during the initial phase of the shaking, due to the elastic behavior of the TDA. The maximum upward heavings (bouncing) of TDA backfill closer to the wall face and farther away from the wall face are both 2 cm (0.8 in.), whereas the maximum upward movement of the sand backfill is 1 cm (0.4 in.).

Figs. 14 and 15 depict the recorded acceleration response time histories of the TDA and the sand backfills, respectively. The accelerometers are placed at 40 cm to the face of the wall in each layer, and one accelerometer is anchored to the box. Table 2 lists the maximum accelerations measured in the four layers in the sand and TDA backfills. Fig. 14 clearly shows the quick attenuation of acceleration from the bottom to the top layers in the TDA backfill: more than 50% reduction of horizontal acceleration is observed when comparing Figs. 14(a and d). Attenuation is not obvious in the sand backfill from the data in Fig. 15. A comparison of each

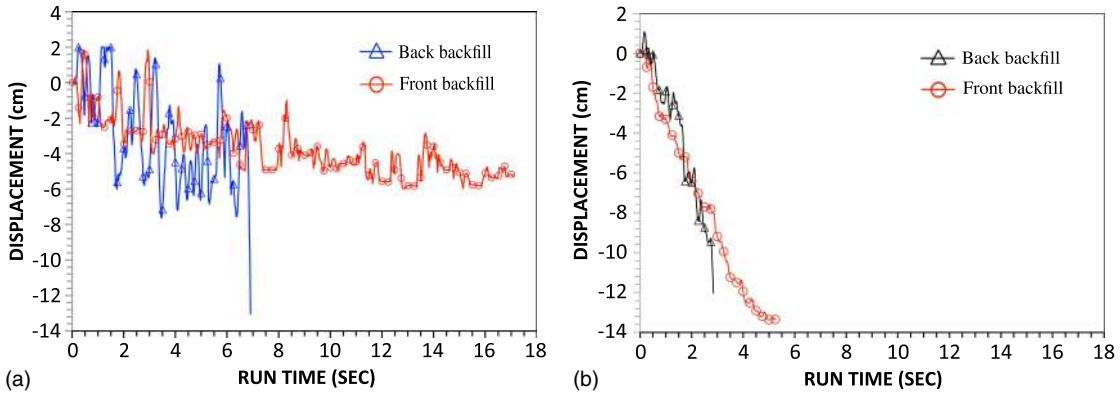

Fig. 13. Seismic vertical settlements of MSE walls: (a) geosynthetically reinforced wall with TDA; (b) geosynthetically reinforced wall with sand

J. Mater. Civ. Eng. 2012.24:1368-1377.

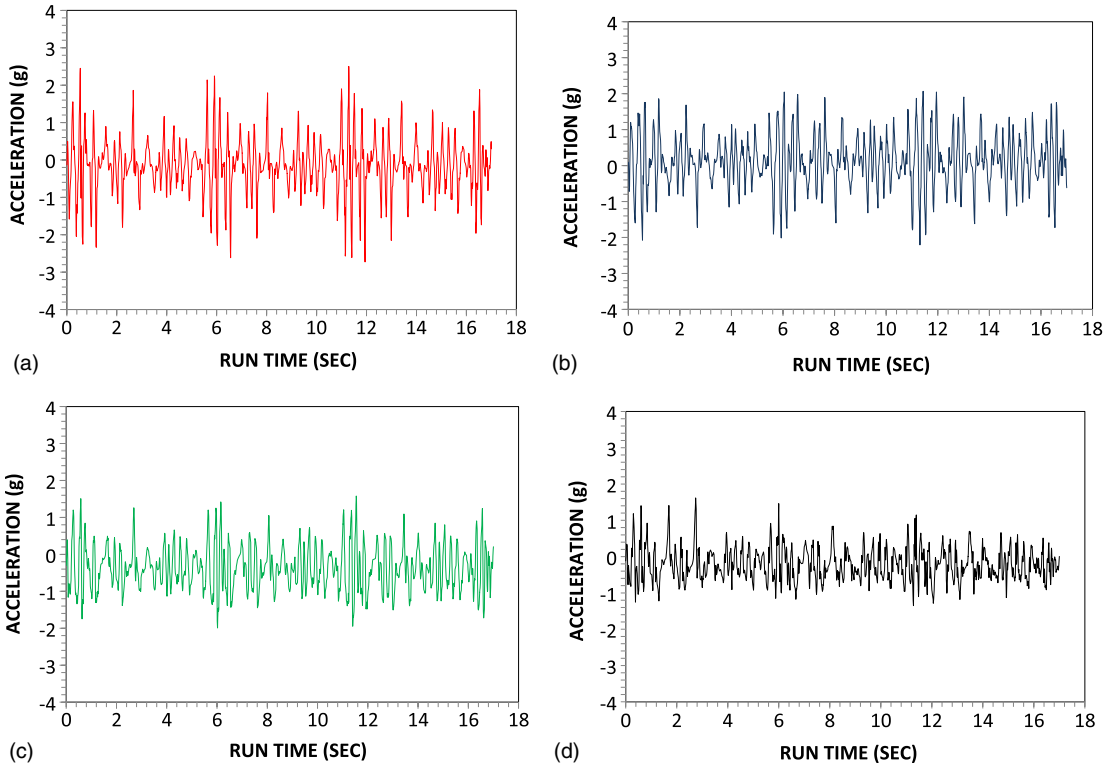

Fig. 14. Accelerations of the TDA backfill (40 cm to the front of the wall): (a) layer 1 (the bottom layer); (b) layer 2; (c) layer 3; (d) layer 4 (the top layer)

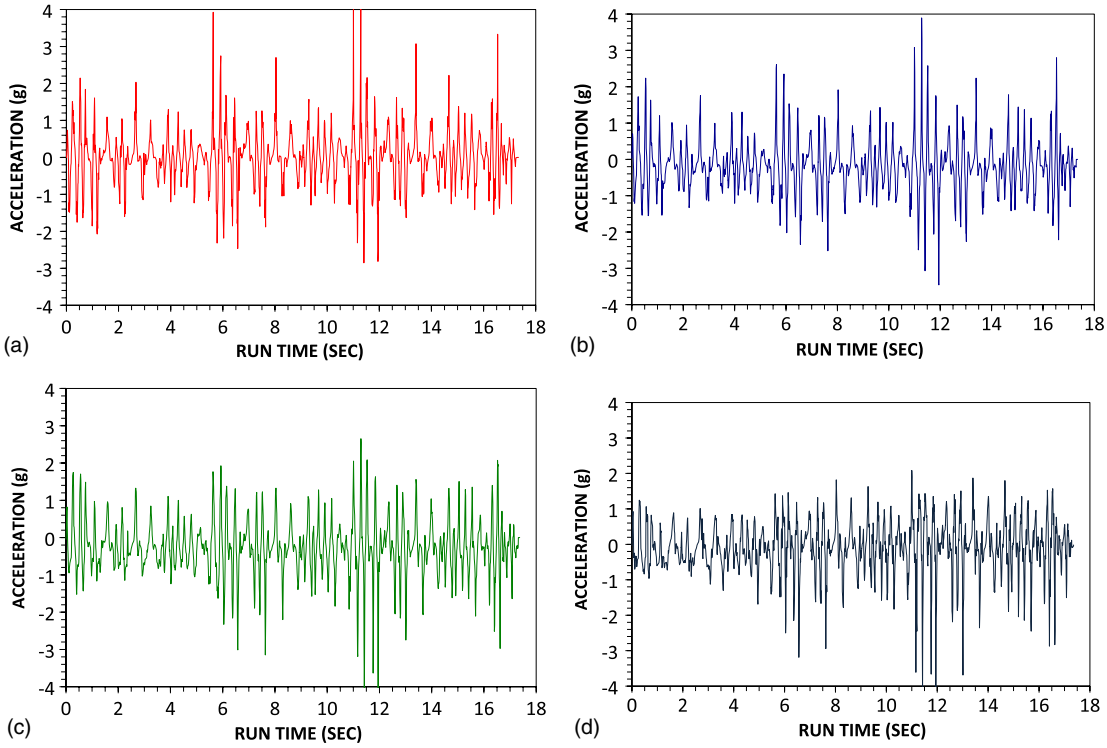

Fig. 15. Accelerations of the sand backfill (40 cm to the front of the wall): (a) layer 1 (the bottom layer); (b) layer 2; (c) layer 3; (d) layer 4 (the top layer)

layer of the TDA and sand backfills clearly shows the consistently smaller acceleration responses in the TDA backfill than in the sand backfill.

Figs. 16 and 17 show the dynamic vertical stresses in the TDA and the sand backfills, respectively. The stresses are recorded by the dynamic soil pressure cells that are embedded at 72 cm from the

J. Mater. Civ. Eng. 2012.24:1368-1377.

Table 2. Maximum Accelerations Measured in the TDA and Sand Backfills (at 40 cm to the Front of the Wall)

Locations of displacement	TDA backfill	Sand backfill
Layer 4 (top)	1.6	2.1
Layer 3	1.6	2.7
Layer 2	2.1	3.9
Layer 1 (bottom)	2.5	5.2

Note: The values are in g.

face of the wall and at the bottom of each layer. Both Figs. 16 and 17 show the expected gradual decrease of stress from the bottom layer to the top layer. Due to the smaller bulk density of the TDA material (529 kg/m^3 or 33 lb/ft^3), the dynamic vertical stresses of the TDA backfill are smaller than those of the sand backfill. When the static pressures in the TDA and sand backfills are compared with the recorded dynamic pressures, both Figs. 16 and 17 indicate that the dynamic pressures are significantly higher than the static pressures. However, this particular observation is uncertain: although each soil pressure transducer was calibrated under static condition using incremental dead weights, the pressure transducers did not respond with accurate readings, even after the calibration. Therefore, the authors have more confidence in comparing the relative readings of different layers than in the absolute recorded stresses of individual layers. Also shown in Fig. 17 is a quick reduction of total stress in the bottom three sand layers (layers 1, 2, and 3) in the initial 2 s. The reason for the extremely high stresses in the initial 2 s of the shaking is unclear to the authors.

The following analysis attempts to explain the mechanisms causing the performance differences of the two types of the geosynthetically reinforced walls.

1. Damping. The test results revealed a higher damping in the TDA backfill. Fig. 14 clearly shows the quick attenuation of acceleration from the bottom to the top layers in the TDA backfill: more than 50% reduction of horizontal acceleration is observed when comparing Figs. 14(a and d). Attenuation is not obvious in the sand backfill from the data in Fig. 15.
2. Elastic characteristics. The modulus of elasticity of the TDA is obtained from the stress-strain curve in Fig. 4. After approximately 8% of strain, the line curves up, displaying higher compression resistance. This is caused by the rigid box bottom containing the TDA and does not represent the true compression characteristic. Therefore, the modulus of elasticity is obtained from the straight line section: 366.7 kN/m^2. The modulus of elasticity (E) of the TDA is significantly lower than that of sand; the typical range of E for sand is 10,000 to 70,000 kN/m^2, depending on its density (Das 2009). The stiffness, which represents the structural property of the retaining wall system, is linearly proportional to the modulus of elasticity. With the same geometrical configuration, the MSE wall with sand backfill has much higher stiffness than the wall with the TDA backfill.
3. Equally important parameters, such as shear strength of the two backfills, natural frequencies of the two model structures, will provide insight to the different seismic responses. Due to the lack of the large direct shear apparatus to accommodate the size of the TDA used in this study, the shear resistance is not measured. Low-amplitude frequency sweep motions on the model walls can help identify their natural frequencies. These parameters are not measured in this study.

The model retaining walls are short (1.6 m in height) and subjected to a small surcharge (15 cm concrete slab, 3.38 kN/m^2). Further study is needed to verify the labotory observations in the field scale. Previous researchers compared the static performances of the TDA walls and sand walls of field scale. Tweedie et al. (1998) conducted experiments of 4.88 m retaining walls using TDA and sand, respectively, and found that the lateral pressure of TDA is 35% less than that of the sand. Humphrey et al. (1998) investigated

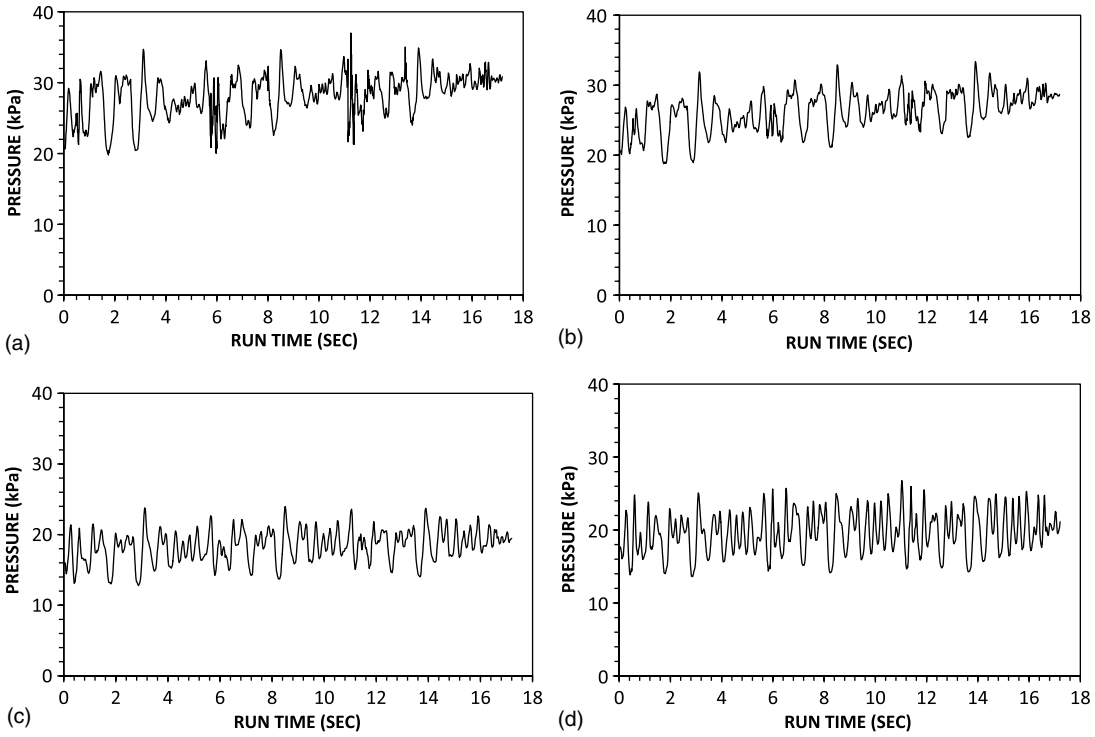

Fig. 16. Dynamic vertical stresses in the TDA backfill: (a) layer 1 (the bottom layer, static pressure = 15.1 kPa); (b) layer 2 (static pressure = 13.0 kPa); (c) layer 3 (static pressure = 10.9 kPa); (d) layer 4 (the top layer) (static pressure = 8.9 kPa)

J. Mater. Civ. Eng. 2012.24:1368-1377.

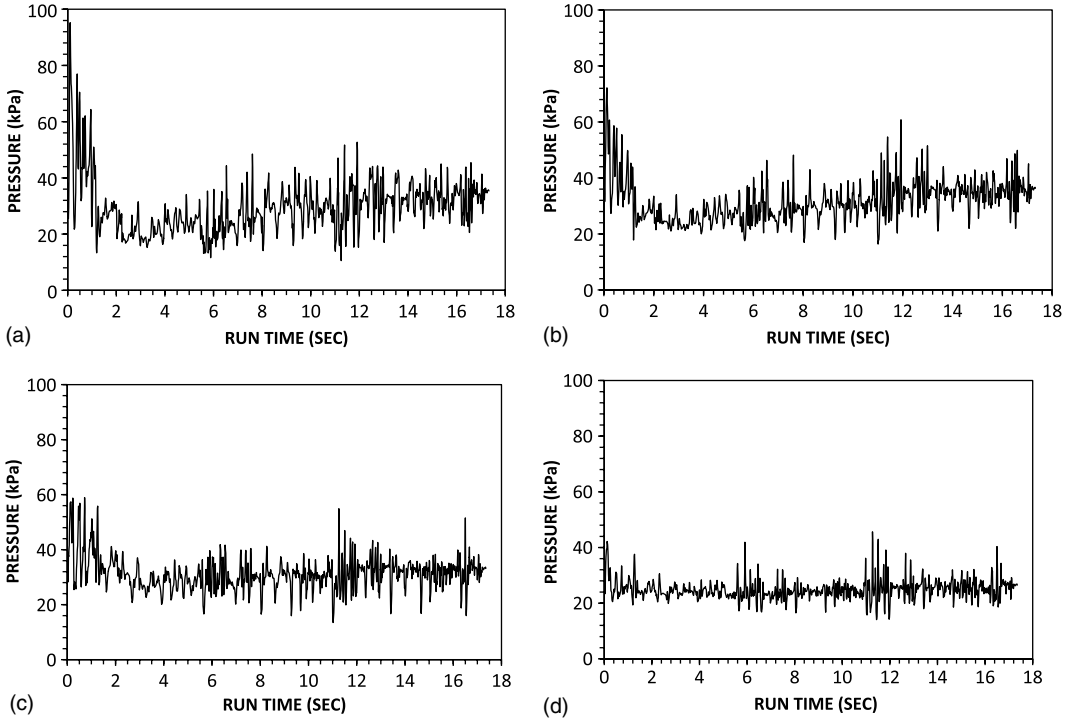

Fig. 17. Dynamic vertical stresses in the sand backfill: (a) layer 1 (the bottom layer)(static pressure = 30.4 kPa);(b) layer 2 (static pressure = 23.7 kPa); (c) layer 3 (static pressure = 17.0 kPa); (d) layer 4 (the top layer) (static pressure = 10.2 kPa)

the bridge abutments using TDA backfills and reported a 50% reduction of lateral pressure. However, the vertical deformations were not reported. Apparently, some of the advantageous performances of TDA walls under static conditions hold up at full scale, but the better seismic performances of the reinforced TDA walls have yet to be verified in the field scale.

Although the comparisons of the seismic behaviors of the two backfills may be valid, the seismic responses of each individual MSE wall may not be extended to the field scale due to the following limitations: (1) the previously discussed observations are based on the reduced-scale walls built in the box, and some scaling issues may be resolved by developing an experimentally calibrated and verified numerical model; (2) the boundary condition of the MSE walls in the box: only a segmental wall is tested, and the boundary condition may influence the seismic responses of the structure; (3) the seismic excitations generated by the shake table are higher than those generally recorded in the field. The reduced-scale experimental results may help the development of a numerical model, which can resolve the scaling and boundary issues and predict the seismic responses of TDA wall and abutments under other earthquake conditions.

Conclusions

This paper presents an experimental research on the seismic responses of geosynthetically reinforced retaining walls with reinforced TDA and compares the responses with the traditional granular backfill under the same simulated earthquake excitations. The research is conducted using reduced-scale shake table tests. Under the same seismic condition and the same wall configurations, the reinforced TDA wall behaves better than the conventional MSE wall. The advantages of TDA backfill over sand include less lateral displacement, less vertical settlement, less acceleration, apparent acceleration attenuation toward the top of the wall, and less static and dynamic stresses in the TDA backfill.

Acknowledgments

This research is funded by the California State University, Fresno. The authors appreciate the support of Steve Scherer, research technician in the Department of Civil and Geomatics Engineering at CSU Fresno, who helped design and build the soil box and set up the data acquisition system. We also thank Cameron Wright of the West Coast Rubber Recycling (Gilroy, CA) for donating the tire derived aggregates, Willie Liew of Tensor International for donating the geogrid and providing the in-situ geogrid installation specifications, and Dr. Mengjia Li of GSE World for donating the geotextile. Prof. Thomas Attard designed and helped build the shake table, and Prof. Jie Han provided advice during the test preparation. The authors sincerely appreciate these support. The authors also appreciate the three anonymous reviewers for providing valuable comments to improve the quality of this manuscript.

References

Accelerated Construction Technology Transfer of the Federal Highway Administration (ACTT). (2005). "ACTT II–The second year report of the Accelerated Construction Technology Transfer Program." FHWA, Washington, DC.

Accelerated Construction Technology Transfer of the Federal Highway Administration (ACTT). (2006). "ACTT III–The third year report of the Accelerated Construction Technology Transfer Program." *Publication No. FHWA-IF-06-028*, FHWA, Washington, DC.

Accelerated Construction Technology Transfer of the Federal Highway Administration (ACTT). (2007). "Accelerated Construction Technology Transfer, building on success." *Publication No. FHWA-IF-07-015*, FHWA, Washington, DC.

Bosscher, P. J., Edil, T. B., and Eldin, N. N. (1992). "Construction and performance of a shredded waste tire test embankment." *Transportation Research Record. 1345*, Transportation Research Board, Washington, DC, 44–52.

J. Mater. Civ. Eng. 2012.24:1368-1377.

Bosscher, P. J., Edil, T. B., and Kuraoka, S. (1997). "Design of highway embankments using tire chips." *J. Geotech. Geoenviron. Eng.*, 123(4), 295–304.

CalRecycle. (2010). ⟨http://www.calrecycle.ca.gov/tires/⟩ (Feb. 18, 2011).

Collin, J. G., Chouery-Curtis, V. E., and Berg, R. R. (1992). "Field observations of reinforced soil structures under seismic loading." *Proc., Int. Symp. on Earth Reinforcement Pract., Earth reinforcement practice*, H. Ochiai, N. Yasufuku, and K. Omine, eds., Vol. 1, Balkema, Rotterdam, Netherlands, 223–228.

Das, B. M. (2009). *Principles of Geotechnical Engineering*, 7th Ed., Cengage Learning, Stamford, CT.

Eliahu, U., and Watt, S. (1991). "Geogrid-reinforced wall withstands earthquake." *Geotech. Fabrics Rep.*, 9(2), 8–13.

Federal Highway Administration. (1997). "User guidelines for waste and byproduct materials in pavement construction." *Publication No. FHWA-RD-97-148*, FHWA, U.S. Department of Transportation, Washington, DC.

Federal Highway Administration. (2006). "Accelerated Construction Technology Transfer (ACTT)." *Publication No. FHWA-HRT-06-054*, FHWA, U.S. Department of Transportation, Washington, DC.

Foose, G. J., Benson, G. H., and Bosscher, P. J. (1996). "Sand reinforced with shredded waste tires." *J. Geotech. Eng.*, 122(9), 760–767.

Hazarika, H., Kohama, E., and Sugano, T. (2008). "Underwater shake table tests on waterfront structures protected with tire chips cushion." *J. Geotech. Geoenviron. Eng.*, 134(12), 1706–1719.

Helwany, M. B., Wu, J. T. H., and Kitsabunnarat, A. (2007). "Simulating the behavior of GRS bridge abutments." *J. Geotech Geoenviron. Eng.*, 133(10), 1229–1240.

Huang, C. C., and Tatsuoka, F. (2001). "Stability analysis of the geosynthetic-reinforced modular block walls damaged during the Chi-Chi Earthquake." *Proc., 4th Int. Conf. on Recent Advances in Geotechnical Earthquake Engineering and Soil Dynamics*, S. Prakash, ed., University of Missouri, Rolla (Mar. 26–31, 2001).

Humphrey, D. N. (1998). "Highway applications of tire shreds." New England Transportation Consortium Rep., University of Maine, Orono, Maine.

Humphrey, D. N., and Manion, W. P. (1992). "Properties of tire chips for lightweight fill." *Proc., Conf. on Grouting, Soil Improvement, and Geosynthetics*, Vol. 2 ASCE, New York, 1344–1355.

Lee, J. H., Salgado, R., Bernal, A., and Lovell, C. W. (1999). "Shredded tires and rubber-sand as lightweight backfill." *J. Geotech. Geoenviron. Eng.*, 125(2), 132–141.

Ling, H. I., Leshchinsky, D., and Chou, N. S. (2001). "Post-earthquake investigation on several geosyntheticic-reinfoced soil retaining walls and slopes during the Ji-Ji earthquake of Taiwan." *Soil Dyn. Earthquake Eng.*, 21, 297–313.

Pando, M., and Garcia, M. (2011). "Tire derived aggregates as a sustainable backfill or inclusion for retaining walls and bridge abutments." *Presentation at the 6th* Geo^{3}T^2 *Conf. and Expo*, Raleigh, NC. ⟨http://www.ncdot.org/doh/preconstruct/highway/geotech/geo3t2/presentations/7A-3.pdf⟩ (Oct. 10, 2011).

Sandri, D. (1994). "Retaining walls stand up to the Northridge earthquake." *Geotech. Fabrics Rep.*, 12(4), 30–31.

Strenk, P. M., Wartman, J., Grubb, D. G., Humphrey, D. N., and Natale, M. F. (2007). "Variability and scale-dependency of tire-derived aggregate." *J. Mater. Civ. Eng.*, 19(3), 233–241.

Tandon, V., Velazco, D. A., Nazarian, S., and Picornell, M. (2007). "Performance monitoring of embankments containing tire chips: Case study." *J. Perform. Constr. Facil.*, 21(3), 207–214.

Tatsuoka, F., Koseki, J., and Tateyama, M. (1997). "Performance of reinforced soil structures during the 1995 Hyogo-ken Nanbu Earthquake." *Earth reinforcement*, H. Ochiai, eds., Balkema, Rotterdam, Netherlands, 973–1008.

Tatsuoka, F., Tateyama, M., and Koleski, J. (1996). "Performance of soil retaining walls for railway embankments." *Soils Found.*, 311–324.

Tsang, H. H. (2008). "Seismic isolation by rubber-soil-mixtures for developing countries." *Earthquake Eng. Struct. Dyn.*, 37, 283–303.

Tweedie, J. J., Humphrey, D. N., and Sandford, T. C. (1998). "Tire shreds as lightweight retaining wall backfill: Active conditions." *J. Geotech. Geoenviron. Eng.*, 124(11), 1061–1070.

Wartman, J., Natale, M. F., and Strenk, P. M. (2007). "Immediate and time-dependent compression of tire derived aggregate." *J. Geotech. Geoenviron. Eng.*, 133(3), 245–256.